

A NEW LINK-LEVEL SIMULATION PROCEDURE OF WIDEBAND MIMO RADIO CHANNEL FOR PERFORMANCE EVALUATION OF INDOOR WLANS

M. Golparvar Roozbahani and E. Jedari

Iran Telecommunication Research Center (ITRC)
P. O. Box: 14155-3961, Tehran, Iran

A. A. Shishegar

Department of Electrical Engineering
Sharif University of Technology
P.O. Box: 11155-9363, Tehran, Iran

Abstract—Inspired by the requirement of proper link simulation methods in performance analysis of communication systems, we present in this paper a recipe for channel implementation in simulation environments. Our focus here is the indoor applications of wireless local-area networks (WLANs). Specifically, we describe a procedure that beginning with statistical description of the channel impulse response leads to an efficient multi-input multi-output (MIMO) channel simulating method for arbitrary antenna configurations at both ends. A sample set of distributions for model parameters are also provided at the 5-GHz band, which is the operating frequency band of IEEE 802.11a, HIPERLAN/2, and the emerging IEEE 802.11n standards, and the corresponding software implementation of the simulator is addressed for public use.

1. INTRODUCTION

Incorporating the concept of multi-input multi-output (MIMO) structure is known to be one of the most appealing candidates for increasing the performance of next generation communication systems [1, 2], including indoor wireless local-area networks (WLANs) [3–8]. In order to accurately estimate the performance of such MIMO WLAN systems and evaluate new proposals, it is essential to have models that predict accurately the behavior of physical propagation channels.

Many performance-evaluation studies appeared in MIMO literature have modeled the MIMO channel matrix with independent and identically distributed (i.i.d.) Gaussian entries, which is an idealistic assumption especially for indoor scenarios. More realistic MIMO channel models can be generally divided into three classes: ray-tracing, scattering, and correlation models [9]. In spite of providing good prediction of the channel behavior, ray-tracing and scattering methods suffer from substantial simulation time and complexity which become prohibitive issues in complex environments. On the other hand, recently published results in [10] cast strong doubts on the validity of correlation-based models. Proposing an efficient yet accurate novel method for implementation of indoor MIMO channels in simulation environments is the goal of this paper.

In spite of a huge interest, there are still a few *indoor wideband MIMO* channel measurements reported in the literature. Simulation methods of these channels based on direct measurements are even fewer. At the 5 GHz band, for example, the publicly available IEEE TGn models [11] are the most convenient tools for MIMO channel simulations. However they have their own limitations; e.g., they are based on single-input single-output (SISO) channel models presented in [12] which do not provide directional information about the propagation channel. In contrast, our proposed procedure for obtaining the MIMO channel model incorporates the angular information of the propagation channel at both ends of the communication link, leading to a double-directional channel model which gives deep insight into the behavior of MIMO channels and allows development of powerful simulation tools that accurately capture the physics of the propagation effects involved.

The rest of this paper is organized as follows. In Section 2, we describe the generic statistical channel models selected for use as the basis of the proposed simulation procedure. This procedure is described in Section 3, beginning with a brief discussion of the normalization issue. In order to have a computationally tractable simulation, it is necessary to have a channel model with fixed tap-spacing. The stage of converting the conventional wideband channel model with random arrival times to such an equivalent channel model with fixed tap-spacings is also described in Section 3 and a block-diagram for channel simulation is given that can be readily implemented in simulation environments. In Section 4, we present typical distributions for the statistical channel model of Section 2 at the 5-GHz band, which is the operating frequency band of several popular standards such as IEEE 802.11a, High Performance Local-Area Networks type 2 (HIPERLAN/2) and the emerging IEEE 802.11n. In

Section 5, a software implementation of the proposed channel simulator in this paper is addressed and then, it is applied to a typical operational scenario of an IEEE 802.11a-based space-division-multiple-access orthogonal-frequency-division-multiplexing (SDMA/OFDM) system. Finally, Section VI concludes the paper.

2. WIDEBAND STATISTICAL CHANNEL MODEL

We distinguish here between the *radio channel* and the *propagation channel* to separate the influence of transmit/receive (Tx/Rx) antennas from the underlying propagation channel. We consider the wideband modeling approach for propagation channel to discriminate between multipath components (MPCs) impinging on the receiver from different directions. In this way, we can adopt the double-directional channel concept [13] in which the angle-of-departure (AOD), angle-of-arrival (AOA), time-of-arrival (TOA), and complex gain of each MPC are specified separately. Moreover, we use the clustering technique for accumulating MPCs [14]. With these assumptions, a generic model for the impulse response of *propagation channel* is proposed as

$$h(\tau, \phi, \theta) = \sum_{k=1}^K \sum_{l=1}^{L_k} (R_k \cdot r_{kl}) \cdot e^{j\varphi_{kl}} \cdot \delta(\tau - T_k - \tau_{kl}, \phi - \Phi_k - \phi_{kl}, \theta - \Theta_k - \theta_{kl}) \quad (1)$$

where $\delta(\cdot)$ is the delta function, K is the number of clusters and L_k is the number of MPCs within the k th cluster. The intercluster parameters T_k , Φ_k , Θ_k and R_k are the TOA of the first arriving MPC, mean AOA, mean AOD and the maximum amplitude of all MPCs within the k th cluster, respectively, while the intracluster parameters τ_{kl} , ϕ_{kl} , θ_{kl} and r_{kl} are the relative values of TOA, AOA, AOD and amplitude of the l th MPC in the k th cluster with respect to T_k , Φ_k , Θ_k and R_k , respectively. φ_{kl} is the phase of the l th MPC in the k th cluster.

The statistical properties of the parameters in (1) may be obtained either through extensive measurement campaigns [14–16] or from ray-tracing simulations [17]. Notwithstanding, the propagation channel model described by (1) has also unifying value. It includes non-clustered models, such as the one in [13], as special cases. When the angular information of propagation channel is not available at either ends of the communication link, it boils down to the non-directional channel model in [14]. With considering AOA only, it reduces to the single-directional channel models in [15] and [16]. Furthermore,

with assuming that spatial and temporal domains are independent, it simplifies to uncorrelated single-directional channel model in [15].

Having modeled the impulse response of *propagation channel*, we can consider the influence of Tx/Rx antennas to get the *radio channel* model. In general, the antennas at both ends of the communication system may be composed of multiple elements, yielding a MIMO system. Supposing far-field scattering to aid classical plane-wave assumption of MPCs at both ends of the link, we propose the MIMO extension of (1) as

$$\mathbf{H}(\tau, \phi, \theta) = \sum_{k=1}^K \sum_{l=1}^{L_k} (\mathbf{A}_{N_r}^{Rx}(\Phi_k + \phi_{kl}))^T \cdot (R_k \cdot r_{kl}) \cdot e^{j\varphi_{kl}} \cdot \mathbf{A}_{N_t}^{Tx}(\Theta_k + \theta_{kl}) \cdot \delta(\tau - T_k - \tau_{kl}, \phi - \Phi_k - \phi_{kl}, \theta - \Theta_k - \theta_{kl}) \quad (2)$$

where $\mathbf{A}_N^x(\alpha) = [P_1^x(\alpha)e^{j2\pi f_c \tau_1^x(\alpha)}, \dots, P_N^x(\alpha)e^{j2\pi f_c \tau_N^x(\alpha)}]$, $x \in \{Tx, Rx\}$, $N \in \{N_t, N_r\}$, and the superscript T denotes matrix transposition. The statistical properties for random parameters in (2) are the same as those in (1), whereas $\tau_i^x(\alpha)$ is the delay time due to finite propagation speed of electromagnetic wave and is a function of the i th antenna element position in the plane, (x_i, y_i) , and the AOD/AOA of the corresponding wave, α , as given by:

$$\tau_i^x(\alpha) = (x_i \cos(\alpha) + y_i \sin(\alpha))/c, \quad i = 1, 2, \dots, N \quad (3)$$

where c is the propagation speed of the plane wavefront. The angular dependency of antenna radiation patterns has also been inserted in (2). $P_n^{Tx}(\alpha)$, $n = 1, \dots, N_t$ represents the angular pattern of the n th element in the Tx array, while $P_m^{Rx}(\alpha)$, $m = 1, \dots, N_r$ is the corresponding parameter of the m th element in the Rx array.

3. CHANNEL SIMULATION PROCEDURE

With the MIMO radio channel model developed in Section 2, we can apply it in the link simulation of communication systems. In order to facilitate the implementation of the model, we discuss two important issues in this section, namely normalizing the channel model and converting it to an equivalent model with fixed tap-spacing.

3.1. Channel Model Normalization

The actual received power to the receiver of a communication system depends on the distance between transmit and receive antennas. Large movements in the location of transmitter and receiver lead to

substantial changes in the path loss of the propagation environment. Effects of path loss in different channel realizations can overshadow interesting channel behavior such as multipath propagation [18]. Therefore, some type of normalization is needed to remove these effects.

Several different normalization approaches have been suggested in the literature and are applicable to our problem at hand; for example, the normalization constant may be computed such that the average power transfer gain between a single transmit and receive antenna is unity. For this purpose, we suggest to scale the amplitude of MPCs such that the expected value of the total power of path gains is unity; i.e.,

$$E \left[\sum_{k=1}^K \sum_{l=1}^{L_k} |R_k \cdot r_{kl}|^2 \right] = 1 \quad (4)$$

where $E[\cdot]$ denotes the expected value.

3.2. Equivalent Channel Model with Fixed Tap-spacing

In order to have a computationally efficient simulation, it is highly desirable that the differential delays between neighboring channel taps be multiples of the simulation sampling time. To this end, let sum up the amplitudes of the MPCs arriving at the same time in (2) to get the channel impulse response between antenna n at the Tx-side and antenna m at the Rx-side as

$$h_{mn}(\tau) = \sum_{i=1}^I c_{mn}[i] \delta(\tau - \tau_i) \quad (5)$$

where $c_{mn}[i]$ and τ_i are the complex amplitude and arrival time of the i th component of h_{mn} respectively. Denoting the continuous-time signals at the position of antenna elements n (at the transmitter) and m (at the receiver) with $x_n(t)$ and $y_m(t)$, respectively, we have:

$$y_m(t) = x_n(t) * h_{mn}(t) \quad (6)$$

where $*$ denotes the convolution operator. In system level simulations, we deal with discrete samples of continuous-time signals with a fixed delay, call it T , between sampling instances. By virtue of the sampling theorem and with assuming that the equivalent lowpass signals are band-limited to $|f| \leq 1/(2T)$, which is a common assumption with sufficient accuracy for practical purposes if the parameter T is chosen

appropriately, we have shown that:

$$y_m[u] = \sum_{v=-\infty}^{\infty} x_n[u-v]g_{mn}[v] \quad (7)$$

where

$$g_{mn}[v] = \sum_{i=1}^I c_{mn}[i] \text{sinc}((vT - \tau_i)/T) \quad (8)$$

and $y_m[u]$ and $x_n[u-v]$ denote respectively $y_m(uT)$ and $x_n((u-v)T)$. Evaluating the infinite sum in (7) gives the same output value at the sampling time as compared to the output of original channel model in (2).

In practical implementation of (7) in a simulation environment, we have to truncate the summing terms to a finite number. Noting that the significant values of $g_{mn}[v]$ appear around $v = 0$, it would be a sensible policy to consider only g_{mn} values in the interval $v = [-V : V]$. By choosing the value of V large enough so that the terms outside the specified interval are negligible, the resulting computational error will be insignificant. Applying the linear transformation of (8) to all links between Tx and Rx arrays, the input-output relationship of radio channel can be efficiently simulated with a finite number of summing terms and identical delays between taps. The resulting truncated tapped delay line model for channel h_{mn} is shown in Fig. 1.

4. A TYPICAL EXAMPLE: MODIFIED SPATIO-TEMPORAL CHANNEL MODEL OF CHONG ET AL. [16]

In order to exemplify the proposed procedure in Sections 2 and 3, we provide in this section a possible set of model parameters to be used for indoor wideband MIMO channel implementation in simulation environments. For this purpose, we have chosen the spatio-temporal channel model proposed by Chong et al. [16] as the basis, which we review briefly in the sequel and modify it so as to be interpretable in the form of (1).

A statistical wideband channel model for 5-GHz band indoor WLAN systems has been proposed in [16] which incorporates both the clustering phenomenon of MPCs and the correlation between the spatial and temporal domains. The model is derived based on single-input multi-output (SIMO) measurement data collected at a carrier

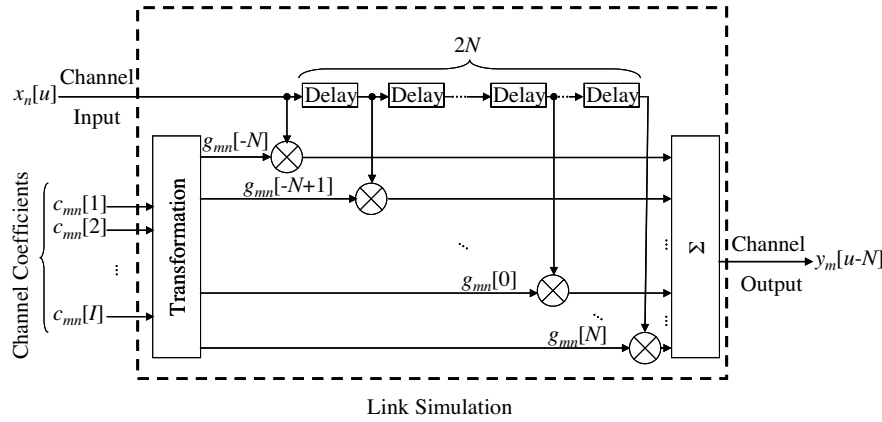


Figure 1. The Proposed simulation model of discrete lowpass equivalent link between antenna n at Tx and antenna m at Rx via tapped delay line.

frequency of 5.2 GHz in three different indoor scenarios, namely line-of-sight (LOS), obstructed-LOS (OLOS) and non-LOS (NLOS) scenarios.

Details of the model parameters and their statistical behavior in different indoor scenarios are given in Table 1. $E(x, \mu)$ and $L(x, \sigma)$ denote respectively the exponential and Laplacian distributions for random variable x , where μ and σ are mean and standard deviation respectively. Notice that the statistics of AOD is not implicitly provided in [16]. Nevertheless, recalling the same basic configuration of reflectors at transmitter and receiver sides in typical indoor applications, it is reasonable to assume that distributions of AOD and AOA are identical. The reasoning is that if the position of Tx and Rx arrays were interchanged in each measurement of AOA, the same value would be measured for AOD, since the spatial paths between Tx and Rx would not be different in these two experiments. Therefore, each measurement of AOA under certain conditions can be viewed as a measurement of AOD under the same conditions too. As a consequence, the same probability distribution would be achieved for AOD as the distribution of AOA. $P_{Inter}(T)$ and $P_{Intra}(\tau)$ in Table 1 are the intercluster and intracluster power-delay density spectrums (PDDS), respectively, while $P_{Inter}(\Phi)$ and $P_{Intra}(\phi)$ are the intercluster and intracluster power-azimuth density spectrums (PADS), respectively. The mean values of R_k and r_{kl} in (1) are respectively proportional to $\sqrt{P_{Inter}(T) \cdot P_{Intra}(\tau)}$ and

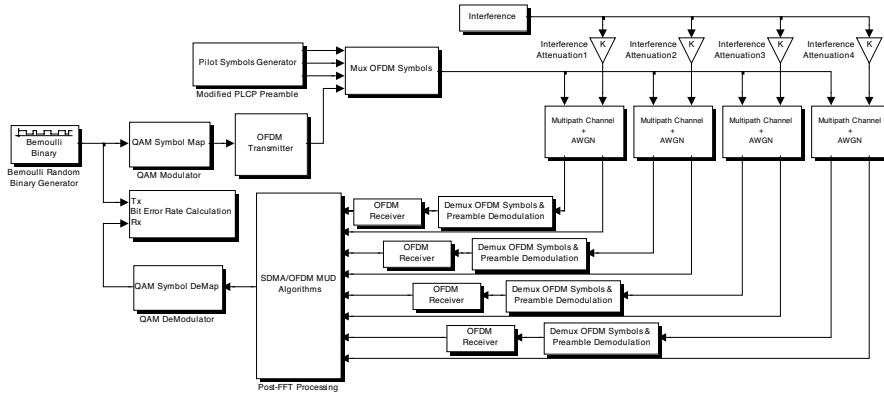


Figure 2. Block diagram of simulated IEEE 802.11a OFDM/SDMA system with 4-elements array antenna.

$\sqrt{P_{Inter}(\Phi) \cdot P_{Intra}(\phi)}$. The proportionality coefficient may be derived from the normalization constraint in (4). This coefficient is constant for the MPCs of a specific channel realization but differs for different realizations. Notice that the statistical distributions of R_k and r_{kl} are not reported in [16]. For this purpose, it seems reasonable to use Rician and Rayleigh distributions for LOS and OLOS/NLOS scenarios, respectively.

5. SIMULATION RESULTS

Once the channel model and the statistical distributions of its parameters are known, different realizations of channel impulse response can be easily generated via computer simulation. Based on the described procedure in this paper, a channel simulating package is developed in the MATLAB[®] 7.0 environment. In this section, we demonstrate a sample scenario where the developed channel simulating package is used for evaluating the communication system performance.

Consider an IEEE 802.11a-based un-coded SDMA/OFDM uplink transmission scenario which consists of four user terminals each equipped with a single antenna and a base station equipped with four-element antenna array. The corresponding simulation model is depicted in Fig. 2, where QPSK scheme is invoked for signal modulation and perfect channel knowledge is assumed at the receiver. The block of *Multipath Channel* in this diagram is implemented via the developed channel simulator.

Table 1. List of channel model parameters and their typical values for different indoor scenarios.

Scenario Parameter	LOS	OLOS	NLOS
K	9	9	7
L_k	Exponentially distributed as $E(L_k, \mu_L)$, where μ_L is		
	1.64	4.09	5.22
φ_{kl}	Uniformly distributed over the range $[0, 360]^\circ$		
T_k	Exponentially distributed as $E(T_k, \mu_T)$, where μ_T , in ns, equals		
	40.88	41.15	52.87
Φ_k (Θ_k has the same distribution)	Has the following conditional distribution $f(\Phi T_k) = \frac{1}{\sqrt{2\pi} \sigma_{\Phi T_k}} \exp\left(-\frac{\Phi^2}{2\sigma_{\Phi T_k}^2}\right)$ where $\sigma_{\Phi T_k}$ is derived from Weibull distribution as $\sigma_{\Phi T_k} = c \cdot \left(\frac{T_k}{a}\right)^{b-1} \cdot \exp\left[-\left(\frac{T_k}{a}\right)^b\right]$ with $a=50.16$, $b=1.54$, $c=67.71$, and T_k value considered in ns.		Uniformly distributed over the range $[0, 360]^\circ$
	Exponentially distributed as $E(\tau_{kl}, \mu_\tau)$, where μ_τ , in ns, equals		
τ_{kl}	13.76	22.00	33.35
ϕ_{kl} (θ_{kl} has the same distribution)	Laplacian distributed as $L(\phi_{kl}, \sigma_\phi)$, where σ_ϕ , in degrees, is		
	3.93	9.03	7.32
$P_{inter}(T)$	Is given by a decaying exponential function. $E(T, \tilde{\alpha}_T)$, where $\tilde{\alpha}_T$, in ns, equals		
	6.52	9.21	10.88
$P_{intra}(\tau)$	Is given by a decaying exponential function $E(\tau, \tilde{\alpha}_\tau)$, where $\tilde{\alpha}_\tau$, in ns, equals		
	13.37	19.09	37.39
$P_{inter}(\Phi)$	Is given by the Laplacian function $L(\Phi, \tilde{\sigma}_\Phi)$, where $\tilde{\sigma}_\Phi = 6.38^\circ$.		Uniformly distributed over the range $[0, 360]^\circ$
	Is given by the Laplacian function $L(\phi, \tilde{\sigma}_\phi)$, where $\tilde{\sigma}_\phi$, in degrees, is		
$P_{intra}(\phi)$	3.31	9.02	9.49

Applying the NLOS channel scenario with model parameters described in Section 4, the bit error rate (BER) performances of

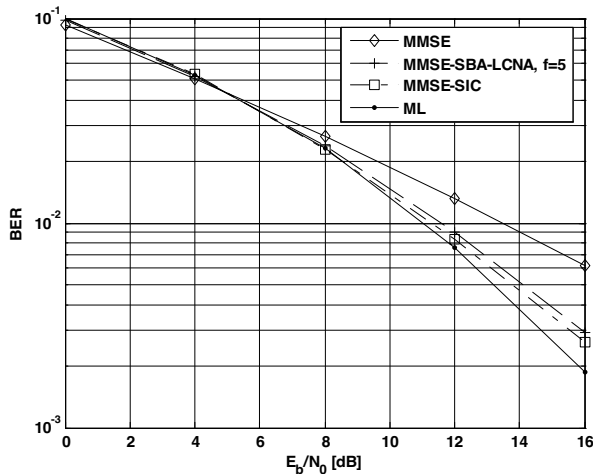


Figure 3. BER Performance comparison of four multi-user detection algorithms (MMSE, MMSE-SIC, MMSE-SBA-LCNA, and ML) applied to the system model of Fig. 2.

some multi-user detection algorithms, namely minimum mean square error (MMSE), MMSE-successive-interference cancellation (MMSE-SIC), two-step reduced complexity maximum likelihood detection (RCMLD) based on sensitive bits algorithm (SBA), and maximum likelihood (ML), are portrayed in Fig. 3. In the first and second steps of SBA-based RCMLD algorithm, MMSE post-FFT multi-user detection (MUD) algorithm and less complex norm approximation (LCNA)-based ML detection algorithm (which we name it as MMSE-SBA-LCNA) are used to correct $f = 5$ sensitive bits. Fig. 3 shows that the MMSE-SIC and MMSE-SBA-LCNA algorithms approximately have the same performance, though the complexity of MMSE-SIC algorithm increases dramatically when the number of users increases [20]. Therefore, with the aid of the link-level simulator providing statistical behavior of the physical radio channel, it may be inferred that when the system performance and algorithm complexity are the two primary benchmarks, MMSE-SBA-LCNA algorithm would be superior to MMSE-SIC algorithm in typical working conditions of the system.

6. CONCLUSION

We established in this paper a new computationally efficient implementation procedure of statistical wideband indoor MIMO channel which is suitable for link level and system level computer

simulations. Based on the knowledge of underlying propagation channel, the way of achieving MIMO channel model was introduced and the implementation procedure was described. Different implementation aspects were discussed and a sample set of statistical distributions for model parameters that are specifically tailored for use in 5-GHz band were presented.

Obviously, the MIMO channel model includes other setups, namely SISO, SIMO and multi-input single-output (MISO) as special cases. Adding this to the fact that our proposed procedure is appropriate for deployment at currently practical frequency bands of indoor applications, we conclude that the proposed simulation method is readily applicable for performance evaluation of a wide range of indoor wireless applications.

REFERENCES

1. Abouda, A. A. and S. G. Häggman, "Effect of mutual coupling on capacity of mimo wireless channels in high snr scenario," *Progress In Electromagnetics Research*, PIER 65, 27–40, 2006.
2. Abouda, A. A., H. M. El-Sallabi, and S. G. Häggman, "Effect of antenna array geometry and ula azimuthal orientation on mimo channel properties in urban city street grid," *Progress In Electromagnetics Research*, PIER 64, 257–278, 2006.
3. Noori, N. and H. Oraizi, "Evaluation of mimo channel capacity in indoor environments using vector parabolic equation method," *Progress In Electromagnetics Research B*, Vol. 4, 13–25, 2008.
4. Hu, C.-F., J.-D. Xu, N. Li, and L. Zhang, "Indoor accurate rcs measurement technique on UHF band," *Progress In Electromagnetics Research*, PIER 81, 279–289, 2008.
5. Xiao, S., J. Chen, B.-Z. Wang, and X.-F. Liu, "A numerical study on time-reversal electromagnetic wave for indoor ultra-wideband signal transmission," *Progress In Electromagnetics Research*, PIER 77, 329–342, 2007.
6. Martinez, D., F. Las-Heras, and R. G. Ayestarán, "Fast methods for evaluating the electric field level in 2D-indoor environments," *Progress In Electromagnetics Research*, PIER 69, 247–255, 2007.
7. Yarkoni, N. and N. Blaunstein, "Prediction of propagation characteristics in indoor radio communication environments," *Progress In Electromagnetics Research*, PIER 59, 151–174, 2006.
8. Talbi, L. and G. Y. Delisle, "Finite difference time domain characterization of indoor radio propagation," *Progress In Electromagnetics Research*, PIER 12, 251–275, 1996.

9. Xu, H., D. Chizhik, H. Huang, and R. Valenzuela, "A generalized space-time multiple-input multiple-output (MIMO) channel model," *IEEE Trans. Wireless Commun.*, Vol. 3, 966–975, May 2004.
10. Weichselberger, W., M. Herdin, H. Özcelik, and E. Bonek, "A stochastic MIMO channel model with joint correlation of both link ends," *IEEE Trans. Wireless Commun.*, Vol. 5, 90–100, Jan. 2006.
11. IEEE 802.11-03/940r4: TGn Channel Models. IEEE. [Online]. Available: [IEEE ftp://ieeewireless@ftp.802wirelessworld.com/11/03/11-03-0940-02-000n-tgn-channel-models.doc](ftp://ieeewireless@ftp.802wirelessworld.com/11/03/11-03-0940-02-000n-tgn-channel-models.doc)
12. Medbo, J. and P. Schramm, "Channel models for hiperlan/2 in different indoor scenarios," *BRAN 3ERJ085B*, March 1998.
13. Steinbauer, M., et al., "The double-directional radio channel," *IEEE Antennas Propagat. Mag.*, Vol. 43, 51–63, Aug. 2001.
14. Saleh, A. and R. Valenzuela, "A statistical model for indoor multipath propagation," *IEEE J. Select. Areas Commun.*, Vol. 5, 128–137, Feb. 1987.
15. Spencer, Q. H., et al., "Modeling the statistical time and angle of arrival characteristics of an indoor multipath channel," *IEEE J. Select. Areas Commun.*, Vol. 18, 347–359, Mar. 2000.
16. Chong, C. C., et al., "A new statistical wideband spatio-temporal channel model for 5-GHz band WLAN systems," *IEEE J. Select. Areas Commun.*, Vol. 21, 139–150, Feb. 2003.
17. Zwick, T., C. Fischer, D. Didascalou, and W. Wiesbeck, "A stochastic spatial channel model based on wave-propagation modeling," *IEEE J. Select. Areas Commun.*, Vol. 18, 6–15, Jan. 2000.
18. Wallace, J. W., et al., "Modeling the indoor MIMO wireless channel," *IEEE Trans. Antennas Propagation.*, Vol. 50, 591–599, May 2002.
19. Enayati, A. R., et al., "Reduced complexity maximum likelihood multiuser detection for OFDM-based IEEE 802.11a WLANs utilizing post-FFT mode," *Proceedings of the IEEE PIMRC'06*, Helsinki, Finland, Sept. 11–14, 2006.